

# Examining ambient noise using co-located measurements of rotational and translational motion

Céline Hadziioannou · Peter Gaebler ·  
Ulrich Schreiber · Joachim Wassermann ·  
Heiner Igel

Received: date / Accepted: date

**Abstract** In the past decade a number of studies have reported the observation of rotational motion associated with seismic events. We report a first observation of rotational motion in the microseismic ambient noise. Information about the seismic phase velocity and source backazimuth is contained in the amplitude ratio of a point measurement of rotation rate and transverse acceleration. We investigate the possibility of applying this method to ambient noise measured with a ringlaser and a broadband seismometer at the geodetic observatory Wettzell in Germany. Using data in the secondary microseismic band, we recover local phase velocities as well as the backazimuth of the strongest noise source for two different dates. These results are confirmed with independent array processing methods.

## 1 Introduction

To fully describe the seismic wave field one needs to measure three components of translational motion, six components of strain and three components of rotational motion. Using seismometers and strain sensors, it is quite an

---

C. Hadziioannou · H. Igel · J. Wassermann  
Department of Earth and Environmental Sciences  
Ludwig-Maximilians-Universität  
Theresienstr. 41  
80333 Munich, Germany  
E-mail: hadzii@geophysik.uni-muenchen.de

P. Gaebler  
GFZ Potsdam

U. Schreiber  
Forschungseinrichtung Satellitengeodäsie  
Fundamentalstation Wettzell  
Sackenriederstrasse 25  
93444 Bad Kötzing, Germany

easy task to measure translational motion and strain. On the other hand, instruments suitable for measuring rotational motions are only starting to make their appearance. In particular, the development of high sensitivity ring laser gyroscopes has made it possible to detect rotational motions excited by seismic events (Stedman et al, 1995; McLeod et al, 1998; Pancha et al, 2000).

One interesting property is that the amplitude ratio of rotational motion around a vertical axis, and the transverse acceleration is twice the horizontal phase velocity (Pancha et al, 2000; Igel et al, 2005; Ferreira and Igel, 2009). Kurrle et al (2010) have shown the possibility and associated difficulties of determining local Love wave dispersion curves using such co-located measurement of both types of ground motion resulting from several seismic events. Igel et al (2007) use the same method to determine the backazimuth of a seismic event, as well. This paper concentrates on the application of the method to ambient noise. We study the origin of oceanic noise sources using two methods: amplitude ratios of co-located measurements of translational and rotational motions recorded at Wettzell, Germany (Schreiber et al, 2009), and  $f - k$  analysis using the Gräfenberg array.

Previously, McLeod et al (1998) and Pancha et al (2000) have shown that ringlaser gyroscopes provide sufficient accuracy to measure seismically induced ground rotations. However, for this study it is important to determine if the Wettzell ringlaser is sufficiently sensitive to continually detect ambient seismic noise. In section 2 we characterize the noise level of the Wettzell ringlaser. In section 5, we determine the noise source direction using only co-located rotational and translational measurements, for two different time periods. The reliability of these results are then assessed using independent array analysis in section 6.

## 2 Characterization of noise on Wettzell Ringlaser

Most ambient noise in the periods from 5 to 20 seconds is generated by the interaction of the atmosphere, ocean waves and the ground. The spectrum of this oceanic noise is dominated by two peaks, the primary microseismic peak at a period around 14 seconds, and the secondary microseismic peak around 7 seconds (e.g. Friedrich et al (1998)). Longuet-Higgins (1950) suggests that the primary microseismic peak originates directly from forcing by strong oceanic waves. The stronger secondary microseisms result from nonlinear interaction of these waves, producing the double-frequency peak. In both cases, the microseismic noise is dominated by fundamental mode surface waves, with Rayleigh waves contributing four times as much energy as Love waves (Friedrich et al, 1998).

Numerous past studies have attempted to localize the origin of primary and secondary microseisms. In this study, we attempt to determine the backazimuthal direction of the strongest microseismic source using co-located rotational motion and transverse acceleration measurements.

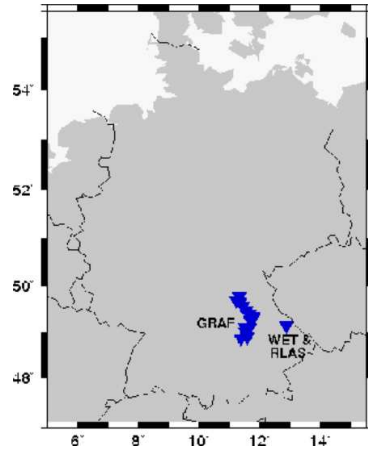


**Fig. 1** Location of Gräfenberg array relative to Wettzell

This study uses rotational motions recorded at the ringlaser of the Wettzell geodetic observatory in Germany (see figure 1). To establish if oceanic microseisms can be detected with this instrument, first its overall noise level is studied. We characterize the noise recorded on the Wettzell ringlaser using the method described in McNamara and Buland (2004). In this method, a statistical analysis is performed on power spectral densities (PSD) taken of 1-hour segments of noise. The analysis yields the probability density function of the noise power as a function of frequency for each station component.

In the course of 2009, the optical mirrors of the ringlaser were replaced, which greatly improved the operation sensitivity of the instrument. In order to compare the noise level before and after this instrument improvement, two months of continuous recordings in the quiet summer periods of 2008 and 2010 were used. The top curve in figure 2 represents the background noise power before the instrument improvement in 2009, the bottom curve represents the same after the improvement. The flat behavior of the top curve is in agreement with the results by Widmer-Schmidrig and Zürn (2009), and is most likely due to instrument noise, not ambient seismic noise.

Figure 2 shows that the overall instrument noise level on the Wettzell ringlaser decreased by a factor of 10 in amplitude after the instrument improvement in 2009. After 2009 (bottom curve), an elevated noise level with respect to the mostly flat instrument noise is visible in the  $[0.1 \text{ } 0.2] \text{ Hz}$  range demonstrates that the Wettzell ringlaser is capable of detecting ambient noise in the secondary microseismic peak. The detection of ambient noise in the primary microseismic peak ( $[0.05 \text{ } 0.1] \text{ Hz}$ ) is more ambiguous. Reason for this are the significantly higher amplitudes excited by the secondary microseisms in comparison to the primary microseisms, making the first easier to observe (Berger et al, 2004). Concretely, while a signal filtered for the primary microseisms exhibits a typical noise level of 0.1 nrad/s, noise amplitudes in the secondary microseismic band reach values of 0.01 nrad/s.

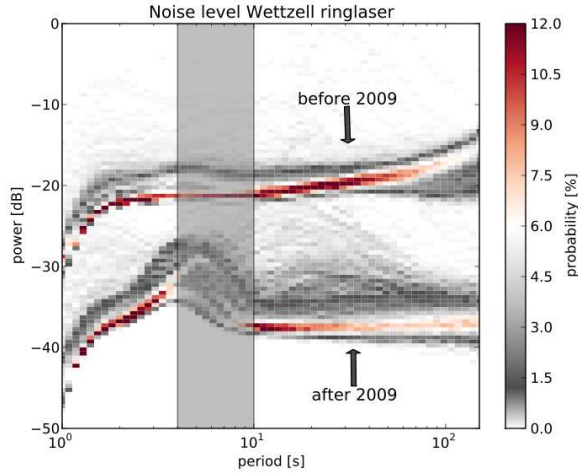


**Fig. 2** Wetzell Ringlaser noise level *before* (top curve) and *after* (bottom curve) an instrument improvement in 2009 (after McNamara and Buland (2004)). Noise levels determined during the summer months of 2008 and 2010, respectively. The colorscale indicates the probability of measuring a certain noise level, the grey shading corresponds to the secondary microseismic band.

Since we have established that the Wetzell ringlaser detects the secondary microseisms, the analyses in the next sections will concentrate on the corresponding frequency band ([0.1 0.2]Hz).

### 3 Theory

For a horizontally polarized plane wave propagating in a homogeneous medium, the similarity between co-located measurements of vertical rotation rate ( $\dot{\omega}_z$ ) and transverse acceleration ( $a_T$ ) is expected to be maximal. The displacement field for an incident wave, transversely polarized along the y-axis, is defined as:

$$\mathbf{u} = [0, A \sin(kx - kct), 0] \quad (1)$$

with amplitude  $A$ , wavenumber  $k$ , phase velocity  $c$  and radian frequency  $\omega$ . The displacement field  $\mathbf{u}$  and rotational motions  $\omega$  are related by:

$$\omega = \begin{pmatrix} \omega_x \\ \omega_y \\ \omega_z \end{pmatrix} = \frac{1}{2} \nabla \times \mathbf{u} = \frac{1}{2} \begin{pmatrix} \partial_y u_z - \partial_z u_y \\ \partial_z u_x - \partial_x u_z \\ \partial_x u_y - \partial_y u_x \end{pmatrix} \quad (2)$$

The rotation rate around a vertical axis  $\dot{\omega}_z$  is then given by:

$$\dot{\omega}_z = \frac{1}{2} k^2 c A \sin(kx - kct), \quad (3)$$

while the transverse acceleration is given by:

$$a_T = \ddot{u}_T = -k^2 c^2 A \sin(kx - kct). \quad (4)$$

From equations (3) and (4), the ratio between the transverse acceleration and the vertical rotation rate is:

$$\frac{a_T}{\dot{\omega}_z} = \frac{-k^2 c^2 A \sin(kx - kct)}{\frac{1}{2} k^2 c A \sin(kx - kct)} = -2c \quad (5)$$

This simple relation means that we can estimate phase velocities from the amplitude ratio co-located measurements of rotational and translational motions.

From equation (5) we can also see that the two signals should have the same waveform, save for the  $-2c$  factor. This property can be used to estimate the source direction of SH-type motions by rotating the horizontal components of the seismometer record along different angles, until their resemblance with the rotational measurements is maximal. The corresponding angle will then point in the direction of the source. Igel et al (2007) and Kurrle et al (2010) have applied this analysis to seismic events. In the next section, it will be applied to ambient noise in the secondary microseismic band.

## 4 Processing

The rotational motion around the vertical axis ( $\dot{\omega}_z$ ) is measured with the Wettzell ringlaser, while the translational ground motion is measured with a STS2 broadband seismometer at the GRSN station WET (see figure 1). This seismometer is located less than 260 meters from the ringlaser, and can thus be considered co-located with the ringlaser for the frequency range investigated in this study.

The signals from both the broadband seismometer and the ringlaser are corrected for instrument response. The seismometer velocity records are differentiated to obtain the acceleration. Finally, all signals are bandpass filtered using a fourth order Butterworth filter in the secondary microseismic band: [0.1 0.2]Hz. All processing is done with the ObsPy toolbox (Megies et al, 2011).

According to equation (5) the amplitude ratio of transverse acceleration and vertical rotation rate gives the apparent phase velocity. The backazimuth of the source can also be determined by rotating the horizontal components of the transverse acceleration until the similarity with the vertical rotation rate signal is maximal.

First, a backazimuth vector is defined with evenly distributed angles between 0 and 360 degrees. The transversal acceleration  $a_T$  is then obtained for each backazimuth angle  $\theta_i$  by rotating the horizontal acceleration components. The similarity between the transversal acceleration and the rotation rate is quantified by calculating the correlation coefficient, which is defined between 0 for no similarity and 1 for a perfect match. The backazimuth angle for the best-fitting transverse acceleration points in the direction of the source.

This process is repeated for a number of overlapping, moving timewindows along the signal, in order to follow the evolution of the main source orientation. The time window length is fixed at a few times the central period  $T_c$ . For each 60 second window, for which the correlation coefficient between the two signals exceeds 0.75, the phase velocity is estimated according to equation 5. This is done by finding the optimal scaling between the rotation rate and the best-fitting transverse acceleration, according to a least squares method.

In the following section, this procedure is tested on a seismic event with known backazimuth, as well as on a day with a strong microseismic source.

## 5 Results

First of all the amplitude ratio method is tested on a seismic event, using two frequency bands: the first centered on the secondary microseismic peak ([0.1 0.2]Hz), the second excluding oceanic microseisms ([0.01 0.03]Hz). On March 11, 2011, the  $M_W$ 9.0 Tohoku-oki event occurred at 05:46 UTC, with a theoretical backazimuth of  $37^\circ$  relative to the Wettzell station. As can be seen in figures 3 and 4, the theoretical backazimuth of the event (red dashed line) is retrieved for both frequency bands, at the time of the main event as well as for a number of aftershocks. The apparent phase velocities attain realistic values as well, of the order of 12 km/s for the steep incoming S-wave arrival, dropping to values around 4 km/s for the surface waves.

In figure 4, with the microseismic peaks excluded, the waveform correlation exceeds 0.75 only at the times of the main event and subsequent aftershocks. However, in figure 3, the waveform correlation stays high throughout the day, even in absence of any seismic events. A maximum correlation is consistently found at a backazimuth of  $300^\circ$ . This suggests that we are observing a microseismic noise source with a backazimuth of  $300^\circ$ . This observation is supported by the work of Friedrich et al (1998), who find a source of secondary microseisms in the Channel region.

The results for a date with a major seismic event are promising, and even seem to show a consistent microseismic source. To test if ambient noise source directions can be found, the method is tested on a date with a strong source of oceanic noise at a known location. On February 26, 2010, the Xynthia storm originated  $30^\circ$  off the coast west of Portugal. A high energy low pressure system like the Xynthia storm significantly increases the height of ocean waves while it is on the open sea or near coastlines. Such increased waveheight is directly linked to the generation of primary and secondary microseismic noise. This particular storm generated strong microseismic activity at a backazimuth of around  $260^\circ$  with respect to Wettzell. In addition to this, on the same date a seismic event occurred in Japan ( $M_W$ 7.0 Ryukyu event), with a theoretical backazimuth of around  $45^\circ$ .

Figure 5 shows the signals for vertical rotation rate and transverse acceleration, the apparent phase velocity obtained using amplitude ratios, the correlation coefficient for each backazimuth as a colorscale and finally the maximum

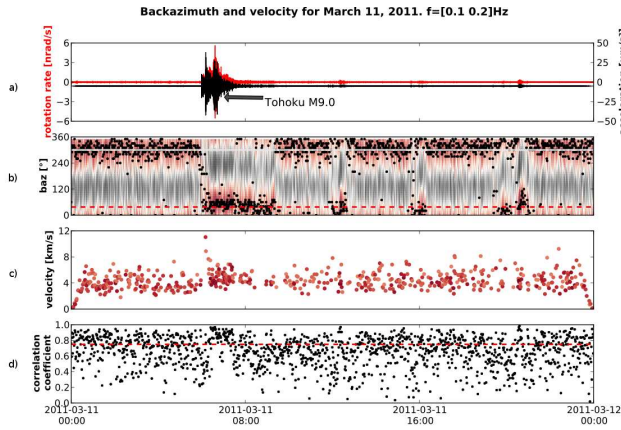


**Fig. 3** Data for March 11, 2011, with the  $M_W$ 9.0 Tohoku-oki event at a backazimuth of  $37^\circ$ . (a) Traces for rotation rate in red and transverse acceleration in black. (b) Backazimuth, with colorscale indicating the correlation coefficient for each backazimuth, and black dot at the maximum correlation coefficient. Median backazimuth is indicated by a white line, the theoretical backazimuth of the Tohoku-oki event by a dashed red line. (c) Phase velocity obtained from amplitude ratio ( $\frac{a_T}{\omega_z}$ ), colorscale corresponds to the correlation coefficient. (d) Maximum correlation coefficient between rotation rate and transverse acceleration.  $f = [0.1 \ 0.2]$ Hz

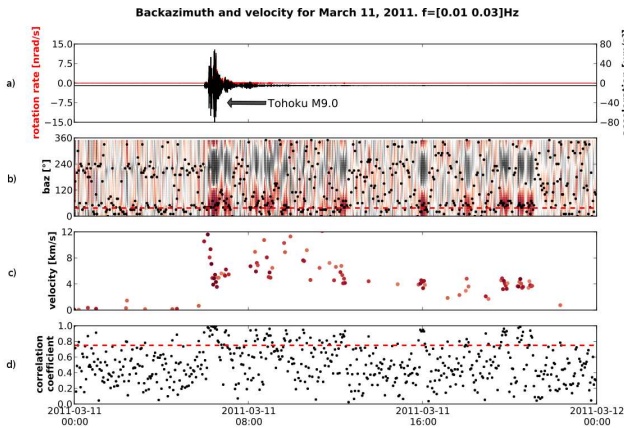


**Fig. 4** As figure 3, but for  $f = [0.01 \ 0.03]$ Hz, excluding the secondary microseismic peak.

correlation coefficient. Over the course of the day, a maximum correlation coefficient (fluctuating around 0.8) can be seen at a backazimuth of  $\sim 270^\circ$ . This corresponds roughly to the South-Western direction, and matches the expected backazimuth of the Xynthia storm ( $260^\circ$ ) closely. In addition to this, the correlation coefficient briefly reaches a maximum value for a backazimuth of  $\sim 50^\circ$  at the time of the Ryuku event.

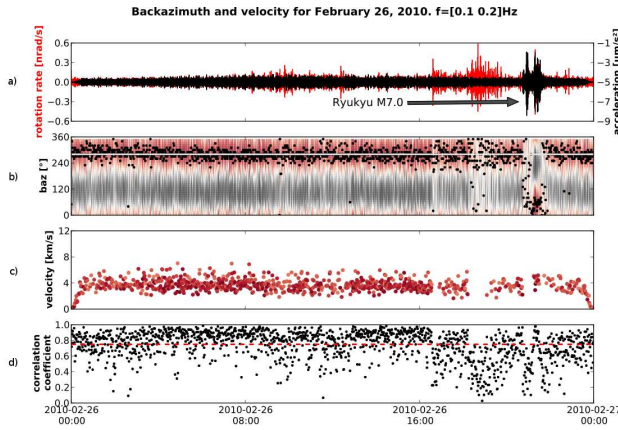


**Fig. 5** One day of data during the Xynthia storm (February 26, 2010). Event is the  $M_W 7.0$  Ryukyu event with a backazimuth of  $45^\circ$ . (a) Traces for rotation rate in red and transverse acceleration in black. (b) Backazimuth, with colorscale indicating the correlation coefficient for each backazimuth, and black dot at the maximum correlation coefficient. Median backazimuth is indicated by a white line. (c) Phase velocity obtained from amplitude ratio ( $\frac{a_T}{\dot{\omega}_z}$ ), colorscale corresponds to the correlation coefficient. (d) Maximum correlation coefficient between rotation rate and transverse acceleration.  $f = [0.1 \ 0.2]$ Hz

Note the higher amplitudes of the ringlaser measurement starting around 17:00. These fluctuations correlate with high wind speeds measured at the meteorological station in Wettzell. There are two possible phenomena at work here. First, strong wind gusts may cause a tilting effect on the ringlaser system, which in turn can affect the measured rotation rate. However, Pham et al (2009) showed, that this effect is negligible in the case of strong teleseismic events and therefore is likely very small in the case of wind influence as well. A second cause could be the strong winds exciting shear forces on the building. These shear forces may be transmitted to the ringlaser system and thus cause significant variations in the measured rotation rate. This sensitivity of the Wettzell ringlaser to local wind speeds does not affect the results in this study, as the consequent decrease of correlation coefficient disqualifies the affected time windows. However, it is important to be aware of this effect.

The results in this section are a strong indication that it is possible to find the direction and apparent phase velocity not only of seismic events, but of ambient noise sources as well, using a point measurement. In the next section, we confirm the observations with an independent analysis using classic array processing methods.

## 6 Comparison to $f - k$ analysis

Following the promising results in the previous section, a frequency-wavenumber analysis is performed on the Gräfenberg array for both dates analysed in sec-



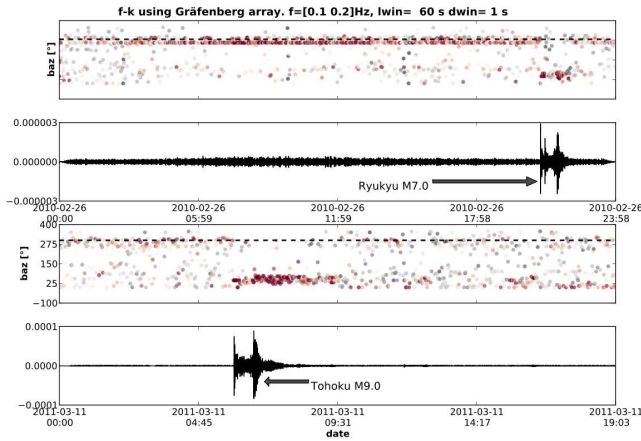


**Fig. 6** Frequency-wavenumber analysis on the Z-component of the Gräfenberg array. Top: during the Xynthia storm (February 26, 2010). Event is the  $M_W$ 7.0 Ryukyu event. Bottom: during the  $M_W$ 9.0 Tohoku-oki event (March 11, 2011). Backazimuth - value obtained with the amplitude ratio ( $\frac{a_T}{\omega_z}$ ) indicated by a dashed black line, colorscale indicates the beampower. Signals are recorded at station GRA1.  $f = [0.1 \ 0.2]$ Hz.

tion 5. This array consists of 13 3-component broadband stations and is located about 50 km west of the Wettzell station (see figure 1). The aperture of the array and the average interstation distance make it suitable to study the microseismic band. Since the array is close to the Wettzell station, we can assume that the same noise sources are observed at both locations. Sources of ambient noise Rayleigh waves are believed to be at approximately the same locations as those of Love waves (Nishida et al (2008)). Therefore, only vertical component records are used in the array analysis.

The data from the Gräfenberg stations are corrected for instrument response, and bandpass filtered for  $[0.1 \ 0.2]$ Hz using a fourth order Butterworth filter. Next, frequency-wavenumber analysis is performed for a moving timewindow. The length of the timewindow is taken such that more than one wavelength of the slowest waves is recorded over the whole array. The beampower maximum is picked for each timewindow, and its backazimuth is represented in figure 6. The backazimuths found using the amplitude ratio method described in section 3 are indicated in the figures as a black dashed line. At both dates, consistent noise sources are detected at backazimuths of  $270^\circ - 280^\circ$ , respectively. As in figure 3, the backazimuth found in figure 6 temporarily shifts to the direction of the Tohoku-oki event and its aftershocks.

The strong agreement with the results from classic frequency-waveform analysis indicates that it is possible to determine the ambient noise source orientation using only a co-located measurement of rotation rate and transverse acceleration.

## 7 Discussion and Conclusion

Recently, improved sensitivity of sensors have made it possible to observe rotational ground motions induced by seismic events. However, the consistent observation of rotational motions in ambient noise has proven difficult. We have shown that, as a result of the instrument improvement in 2009, the Wettzell ringlaser can detect rotational motions in microseisms in the secondary microseismic band ([0.1 0.2]Hz).

A co-located measurement of rotation rate and transverse acceleration lead to a backazimuth estimation as well as one for the apparent phase velocity. By applying the method detailed in section 3, a consistent high correlation between rotation rate and transverse acceleration signals is found in the secondary microseismic band, which is not present at different frequencies. This high correlation points to a noise source at a backazimuth of  $300^\circ$ . Testing the same method on a different date, with a strong noise source (the Xynthia storm) yields a backazimuth close to the theoretical value of  $\sim 270^\circ$ . The apparent velocities found with this method correspond to the expected local values.

Finally, these results are checked against classic array beamforming analysis. For practical reasons, this f-k analysis was performed on vertical component records. However, since both ambient noise Rayleigh and Love waves are believed to be generated in the same areas (Nishida et al (2008)), the results can still be compared. Using array beamforming techniques, the same main source backazimuths are found as with the amplitude ratio method in section 5.

**Acknowledgements** We gratefully acknowledge support from the European Commission (Marie Curie Actions, ITN QUEST, [www.quest-itn.org](http://www.quest-itn.org)).

## References

- Berger J, Davis P, Ekström G (2004) Ambient earth noise: a survey of the global seismographic network. *Geophys Res Lett* 109:B11,307
- Ferreira A, Igel H (2009) Rotational motions of seismic surface waves in a laterally heterogeneous earth. *Bull Seismol Soc Am* 99(2B):1429
- Friedrich A, Krüger F, Klinge K (1998) Ocean-generated microseismic noise located with the gräfenberg array. *Journal of Seismology* 2(1):47–64
- Igel H, Schreiber U, Flaws A, Schuberth B, Velikoseltsev A, Cochard A (2005) Rotational motions induced by the m8. 1 tokachi-oki earthquake, september 25, 2003. *Geophys Res Lett* 32:L08,309
- Igel H, Cochard A, Wassermann J, Flaws A, Schreiber U, Velikoseltsev A, Pham Dinh N (2007) Broad-band observations of earthquake-induced rotational ground motions. *Geophys J Int* 168(1):182–196, DOI 10.1111/j.1365-246X.2006.03146.x, URL <http://blackwell-synergy.com/doi/abs/10.1111/j.1365-246X.2006.03146.x>

- Kurrle D, Igel H, Ferreira AMG, Wassermann J, Schreiber U (2010) Can we estimate local Love wave dispersion properties from collocated amplitude measurements of translations and rotations? *Geophys Res Lett* 37(4):1–5, DOI 10.1029/2009GL042215, URL <http://www.agu.org/pubs/crossref/2010/2009GL042215.shtml>
- Longuet-Higgins M (1950) A theory of the origin of microseisms. *Philosophical Transactions of the Royal Society of London Series A Mathematical and Physical Sciences* 243(857):1–35
- McLeod D, Stedman G, Webb T, Schreiber U (1998) Comparison of standard and ring laser rotational seismograms. *Bull Seismol Soc Am* 88(6):1495
- McNamara DE, Buland RP (2004) Ambient Noise Levels in the Continental United States. *Bull Seismol Soc Am* 94(4):1517–1527
- Megies T, Beyreuther M, Barsch R, Krischer L, Wassermann J (2011) Obspy—what can it do for data centers and observatories? *Annals of Geophysics* 54(1):47–58
- Nishida K, Kawakatsu H, Fukao Y, Obara K (2008) Background Love and Rayleigh waves simultaneously generated at the Pacific Ocean floors. *Geophys Res Lett* 35(16):1–5, DOI 10.1029/2008GL034753, URL <http://www.agu.org/pubs/crossref/2008/2008GL034753.shtml>
- Pancha A, Webb TH, Stedman GE, McLeod DP, Schreiber KU (2000) Ring laser detection of rotations from teleseismic waves. *Geophys Res Lett* 27(21):3553, DOI 10.1029/2000GL011734, URL <http://www.agu.org/pubs/crossref/2000/2000GL011734.shtml>
- Pham N, Igel H, Wassermann J, Kaser M, de La Puente J, Schreiber U (2009) Observations and modeling of rotational signals in the p coda: constraints on crustal scattering. *Bull Seismol Soc Am* 99(2B):1315
- Schreiber K, Hautmann J, Velikoseltsev A, Wassermann J, Igel H, Otero J, Vernon F, Wells J (2009) Ring laser measurements of ground rotations for seismology. *Bull Seismol Soc Am* 99(2B):1190
- Stedman G, Li Z, Bilger H (1995) Sideband analysis and seismic detection in a large ring laser. *Applied Optics* 34(24):5375–5385
- Widmer-Schmid R, Zürn W (2009) Perspectives for ring laser gyroscopes in low-frequency seismology. *Bull Seismol Soc Am* 99(2B):1199